CONFIDENTIAL

Copy 394
RM E54L20a

RESEARCH MEMORANDUM

COMPRESSOR-BLADE VIBRATION AND PERFORMANCE IN A J47-23 TURBOJET ENGINE UNDER CONDITIONS OF ROTATING STALL

By Morgan P. Hanson, Donald F. Johnson, and André J. Meyer, Jr.

Lewis Flight Propulsion Laboratory
Cleveland, Ohio

NATIONAL ADVISORY COMMITTEE FOR AERONAUTICS

WASHINGTON

June 3, 1955

CONFIDENTIAL

NATIONAL ADVISORY COMMITTEE FOR AERONAUTICS

RESEARCH MEMORANDUM

COMPRESSOR-BLADE VIBRATION AND PERFORMANCE IN A J47-23 TURBOJET ENGINE UNDER CONDITIONS OF ROTATING STALL

By Morgan P. Hanson, Donald F. Johnson, and André J. Meyer, Jr.

SUMMARY

An investigation was made of a J47-23 turbojet engine to determine the compressor-blade vibration and performance under conditions of rotating stall. Resistance-wire strain gages were used to measure the vibration of selected blades from each of the first seven stages and hot-wire anemometers were used to determine the rotating stall. One to nine stall zones were measured, with the seven stall in predominance. Under normal operation, the maximum vibratory stress measured was ±26,200 psi in the second-stage blades. However, under simulated rapid acceleration conditions, a stress of ±60,000 psi was measured in the second stage. Compressor performance is presented for the operating conditions investigated.

INTRODUCTION

A serious problem in the development of the turbojet engine is that of compressor-blade failures due to vibration fatigue. In the past, it was realized that the wakes from stationary elements could set up discontinuities in the air flow, thereby establishing periodic fluctuations in resonance with rotor-blade frequencies. By careful design, this source of excitation has been generally eliminated. Recently, in the study of compressor dynamics several investigators have found that stall of the compressor-blade rows resulted in the formation of low-flow zones in the compressor annulus (ref. 1). These low-flow zones established themselves in a seemingly equispaced pattern and propagated at a fractional rate of compressor speed in the direction of compressor rotation; hence, the name rotating stall. Generally, rotating stall was found to occur from 50 to 70 percent of the design speed of the compressor. An explanation of the stall propagation at intermediate speeds is given by the fact that the design inlet-to-exit area ratio of the compressor is too large to allow

off-design operation in all stages without stall. The existence of the low-flow zones suggests the possibility of periodic excitations relative to the rotating compressor blades. Presumably, if the relative stall frequency is equal to or a harmonic of any blade frequency, resonant vibration can occur. In resonant vibration, the magnitude of the vibration is governed by the damping in the blade system and the energy of the exciting force. Some variation in the damping is experienced because of aerodynamic forces, stress of the blade material, and mechanical losses, but is generally low and limited physically (ref. 2). It remains that, if the exciting energy becomes sufficiently great, vibration fatigue can occur. The object of the investigation reported herein was to determine the compressor-blade vibration and performance under conditions of rotating stall.

The investigation was conducted in a sea-level test stand at the NACA Lewis laboratory. The engine was operated in an as-received condition and was equipped with a variable exhaust nozzle to establish desired engine conditions. Rotating stall was determined by the use of hot-wire anemometry, and strain gages were used to measure blade vibrations. Temperature and pressure instrumentation was provided for compressor performance computation.

APPARATUS AND PROCEDURE

Apparatus

Turbojet engine. - The engine used in the investigation was a J47-23 rated at 6060 pounds thrust at 7950 rpm with a turbine-discharge temperature of 1245° F. The engine was equipped with a variable exhaust nozzle for establishing rated engine conditions. A bellmouth provided uniform air flow to the engine inlet. Four temperature-pressure probes were located radially and 90° apart in the straight section of the bellmouth. Compressor-discharge temperature and pressure were also measured with four probes at 90° locations.

Strain-gage instrumentation. - Individual compressor-blade vibration was detected by the use of two resistance-wire strain gages cemented to either side of selected blades at their midchord section and as close to the blade base as possible. The two active strain gages were connected to two balance gages to form a bridge circuit on the compressor rotor. Four blades in each of the first seven stages of the compressor were instrumented with strain gages. Electrical continuity for the strain gages to the power supply and recording oscillograph was provided by the use of special slip rings. The strain-gage application and instrumentation is fully explained in reference 3.

Hot-wire anemometer. - The hot-wire anemometer was of the constant-temperature type and was similar to that described in reference 4. The hot-wire probes were provided with 0.1-inch lengths of 0.001-inch-diameter wire. Radial surveys were made possible by the use of probe actuators that traversed the stator passage. Provision was made for hot-wire anemometers in each of the first seven stator sections. The first stator was provided with three hot-wires placed to allow data reduction from angular displacements of 30°, 60°, and 90° between some pair of the wires.

Procedure

To establish a particular engine condition, the exhaust nozzle was adjusted to produce a predetermined turbine-discharge temperature at a given speed. Figure 1 is a plot of the turbine-discharge temperature against engine speed. Four different exhaust-nozzle settings were investigated and are subsequently referred to as open, rated, closed A, and closed B. The rated nozzle setting corresponded to that required to produce the rated turbine-discharge temperature at rated speed as established by the manufacturer. The closed nozzle settings were intended to simulate conditions such as experienced in rapid accelerations not normally allowed by the standard engine controls system.

During investigation of rotating stall and compressor-blade vibration, data were taken throughout transient as well as steady-state operation. Blade-vibration and stall data were deduced from the oscillograph records. Two hot-wire anemometers were used in the first-stage stator row to permit determination of the number of stall zones by the procedure outlined in reference 1. In addition, rotating-stall signals from the second to the seventh stage were recorded for comparison purposes.

Compressor performance was computed from average total-pressure and -temperature measurements at the compressor inlet and discharge sections. Measurements were made under steady-state operation at specific points throughout the speed range of the engine and with the exhaust nozzle open, rated, and closed A.

DISCUSSION AND RESULTS

Rotating Stall

Analysis of the recorded hot-wire oscillograms revealed the existence of rotating stall in the compressor annulus. The stall extended in an axial direction throughout the instrumented compressor stages, and propagated in the direction of compressor rotation at approximately

50 percent of rotor speed. One to nine stall zones were observed under varied operation, although the eight- and nine-zone stalls were of limited duration and infrequent occurrence. Figure 2 shows the extent of the one to seven stall zones with respect to engine speed at various exhaust-nozzle settings. The open ends of the bars in the graph indicate either the lack of sufficient data or the inability to establish the extremity of the stall from the data. It is seen that the extent of the rotating stall range was influenced primarily by the nozzle setting. Also, the upper extremity of the stall occurred at a higher speed during acceleration than during deceleration. Similarly, the lower extremity occurred at a higher speed during acceleration.

The occurrence of a specific stall pattern varied, approximately depending upon engine speed and the nozzle setting. Once either a one- or two-zone stall pattern was established, it would maintain itself until the engine speed was changed to introduce another stall pattern. However, with three to seven stall zones the stall pattern was continually changing, with a given stall zone remaining only momentarily. Even so, it was observed that certain stall patterns predominated, and again were influenced by nozzle setting. Closing the nozzle also sustained the predominant stalls. The haphazard manner of the stall pattern accounts for the overlapping of the stall zones and may account for the exclusion of certain stall zones in figure 2. At the lower speed range of the rotating stall, it was difficult to establish the transition from rotating stall to random flow fluctuations. In contrast, at the upper extremity of the stall range, once rotating stall ceased, the anemometer no longer picked up significant flow disturbances.

Figure 3 is a plot of the various stall frequencies as a function of engine speed. The full extent of the range is presented, irrespective of nozzle setting. The dashed portion of the curves corresponds to the open ends of the bar graph in figure 2. The dashed curves for eight- and nine-zone stalls indicate an approximation in the extent and frequency change with speed. Sufficient data were available to establish the frequency in a limited speed range; however, beyond this range the eight- and nine-zone stalls were in existence for such a short duration that it was impossible to make a precise determination of frequency.

Compressor-Blade Vibration

Vibration was observed in all strain-gaged blades of the first seven stages. The strain-gage traces showed appreciable stage-to-stage variation in vibratory stress, with the greatest amplitude being measured in the second-stage blades. A plot of vibratory stress against engine speed for the second-stage blades is presented in figure 4, showing the maximum vibrations for different nozzle settings. It is seen that under normal

operating conditions, that is, rated nozzle, the maximum measured vibratory stress was ±26,200 psi. However, by closing the nozzle, a maximum vibration representing ±60,000 psi was measured, indicating that under abnormal operating conditions difficulties might be encountered from fatigue of the blade material.

To consider rotating stall as a possible source of compressor-blade vibration excitation, the rotating-stall frequency relative to the blade frequencies must be computed. Since the rotating stall zone frequency f_s is propagating in the same direction as compressor rotation, the frequency f_s' relative to the blades can be computed by the following formula:

$$f_s' = N\lambda - f_s$$

where

N rotor speed, rps

λ number of stall zones

When the relative stall zone frequency is known, it is possible to correlate stall frequency with the blade frequency. This can be done by the use of a critical speed diagram. Figure 5(a) is a critical speed diagram showing the calculated variation of the blade natural frequency with rotor speed. The calculation was based on the method presented in reference 5. The solid lines passing through the origin are order lines that are exact multiples of the coordinates in common units and that show possible sources of resonant vibration. The relative stall frequencies for one- to nine-stall zone patterns are included to determine the intersections with the blade natural frequencies. It is seen that the fundamentals of the one to five relative stall frequencies lie below the natural frequency of the compressor blades. However, the harmonics of the fundamental frequencies intersect the blade frequencies and could induce resonant vibration. The fundamental frequencies of the six to nine stalls intersect the blade frequencies of the first and second stages at various engine speeds, revealing potential resonant vibration. Figure 5(b) shows a section of the critical speed diagram with actual data points for the first stage and for each of the four instrumented blades in the second stage. Since no measurement was made of the exciting force, the severity of the resonance can only be based on the magnitude of the resulting vibration.

As was mentioned previously, certain stall zones predominated. This was particularly true of the seven stall zones when operating the engine in the vicinity of 5200 rpm with the nozzle closed. At approximately this speed and nozzle setting, the second-stage blade vibration was

±60,000 psi because the blade frequency was in resonance with the fundamental of the relative seven-zone stall frequency. With engine speed remaining the same and the nozzle set at rated, the vibratory stress was reduced appreciably. From figure 2, it can be seen that the seven-zone stall range for the rated nozzle falls short of the resonance speed (approx. 5200 rpm); hence, the reduced vibration. This can be physically observed in figure 6 where the two oscillograms recorded at the same speed (5250 rpm) show different stall patterns for rated and closed nozzle. At this speed with rated nozzle, the seven-zone stall pattern is not in evidence (fig. 6(a)). However, with the closed nozzle, the seven-zone stall pattern predominates and is more sustained (fig. 6(b)). No direct comparison can be made of the oscillograms as to amplitude because there was a difference in attenuation of the signals. The intersection of the seven stall zones and the first-stage blade natural frequency, at approximately 4800 rpm, induced a vibratory stress of ±11,000 psi. Observation of the oscillograms indicated that at 4800 rpm the seven-zone stall had diminished in strength and prominence, which likely explains the limited stress value. Again, this is probably the sole explanation of the low stress due to the six-, eight-, and nine-zone stall excitations in the first- and second-stage blades.

Table I is a summary of the maximum vibratory stresses occurring in each of the seven stages at engine speeds where the stresses predominated, irrespective of operating conditions. Also included is the source of excitation as determined from an analysis of the data. It can be seen that rotating stall is the main source of excitation either at the fundamental frequency or at harmonics of the fundamental. With the exception of the second stage, the peak vibrations ranged from ±5200 to ±17,500 psi in the remaining six stages.

Compressor Performance

Compressor performance is presented for the operating conditions investigated. Figure 7 shows the variation of compressor efficiency with engine speed for open, rated, and closed A nozzle under steady-state operation. Figure 8 is the compressor performance map showing the plot of pressure ratio against weight flow with efficiency and speed parameters for the various nozzle settings. The performance with the closed-nozzle operation is terminated at about 6000 rpm because of approaching limiting turbine temperatures.

SUMMARY OF RESULTS

An investigation was made of a J47-23 turbojet engine to determine the compressor-blade vibration and performance under conditions of rotating stall. Resistance-wire strain gages were used to measure the vibration of selected blades in the first seven stages, and hot-wire anemometers were used to determine the rotating stall. Compressor performance was computed from pressure and temperature data in a speed range from rated to approximately 40 percent of rated. One- to seven-zone stalls were measured with eight- and nine-zone stalls occurring sporadically. The stall pattern in the one- or two-zone stalls, when once established, would maintain itself until a change in engine speed caused the occurrence of another pattern. In the speed range where three- to nine-zone stalls appeared, the pattern continually changed in number with the seven-zone stall in predominance. The predominance was accentuated by closing the nozzle. Under normal operation with rated nozzle, a maximum vibratory stress of ±26,200 psi was measured in the second stage. However, by closing the nozzle to simulate at constant speed the conditions that exist during very rapid acceleration, a stress of ±60,000 psi resulted in the second stage. These maximum vibratory stress values were due to the second-stage blade frequency being in resonance with the fundamental of the relative seven-zone stall frequency occurring at approximately 5200 rpm. In the remaining stages, the maximum stresses ranged from ±5200 to ±17,500 psi and were excited mainly by the fundamental or a harmonic of a particular stall frequency.

Compressor performance is presented for the operating conditions investigated showing the effect of operating variables on compressor efficiency, pressure ratio, and weight flow.

Lewis Flight Propulsion Laboratory
National Advisory Committee for Aeronautics
Cleveland, Ohio, December 15, 1954

REFERENCES

1. Huppert, Merle C.: Preliminary Investigation of Flow Fluctuations During Surge and Blade Row Stall in Axial-Flow Compressors. NACA RM E52E28, 1952.

2. Hanson, M. P., Meyer, A. J., Jr., and Manson, S. S.: A Method of Evaluating Loose-Blade Mounting as a Means of Suppressing Turbine and Compressor Blade Vibration. Proc. Soc. Exp. Stress Analysis, vol. 10, no. 2, Nov. 1952, pp. 103-116.

3. Meyer, André J., Jr., and Calvert, Howard F.: Vibration Survey of Blades in 10-Stage Axial-Flow Compressor. II - Dynamic Investigation. NACA RM E8J22a, 1949. (Supersedes NACA RM E7D09.)

4. Laurence, James C., and Landes, L. Gene: Auxiliary Equipment and Technique for Adapting the Constant-Temperature Hot-Wire Anemometer to Specific Problems in Air-Flow Measurements. NACA TN 2843, 1952.

5. Timoshenko, S.: Vibration Problems in Engineering. Second ed., D. Van Nostrand Co., Inc., 1937, p. 386.

TABLE I. - MAXIMUM VIBRATORY STRESSES

Stage	Peak stress, ±psi	Engine speed, rpm	Source of excitation
1	9,200	4400	9 Stall
	11,000	4800	7 Stall
	16,000	5200	6 Stall
2	24,000	4650	9 Stall
	60,000	5230	7 Stall
3	17,500	4925	1st Harmonic 4 Stall
	17,000	5250	3rd Harmonic 2 Stall
4	15,500	4800	5th Order
	13,200	5180	1st Harmonic 5 Stall
5	12,000	4800	6th Order
	11,000	5000	2nd Harmonic 4 Stall
	10,800	5180	1st Harmonic 6 Stall
6	6,400	4930	8th Order
7	5,200	5600	9th Order

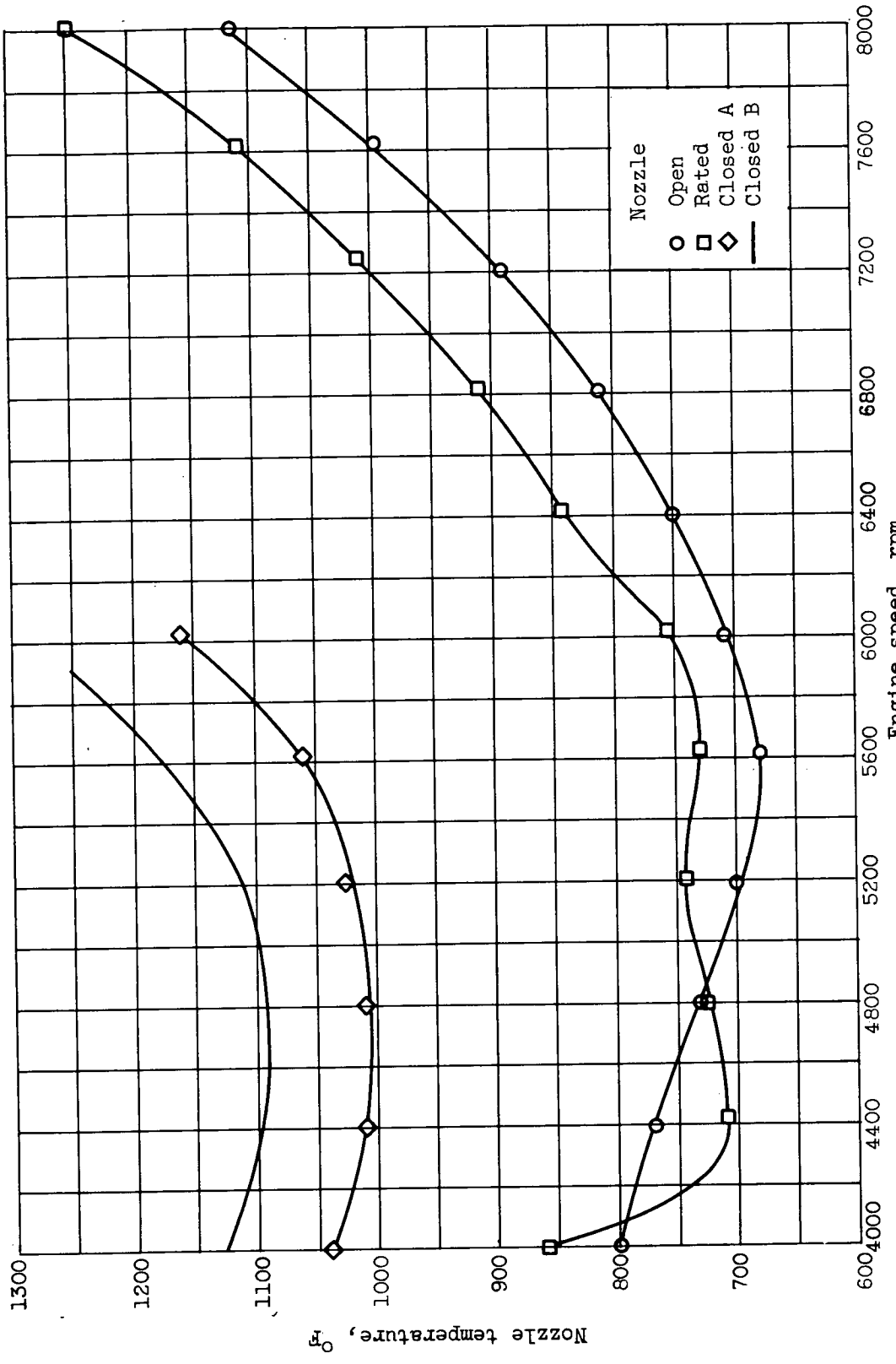

Figure 1. - Nozzle temperature against engine speed.

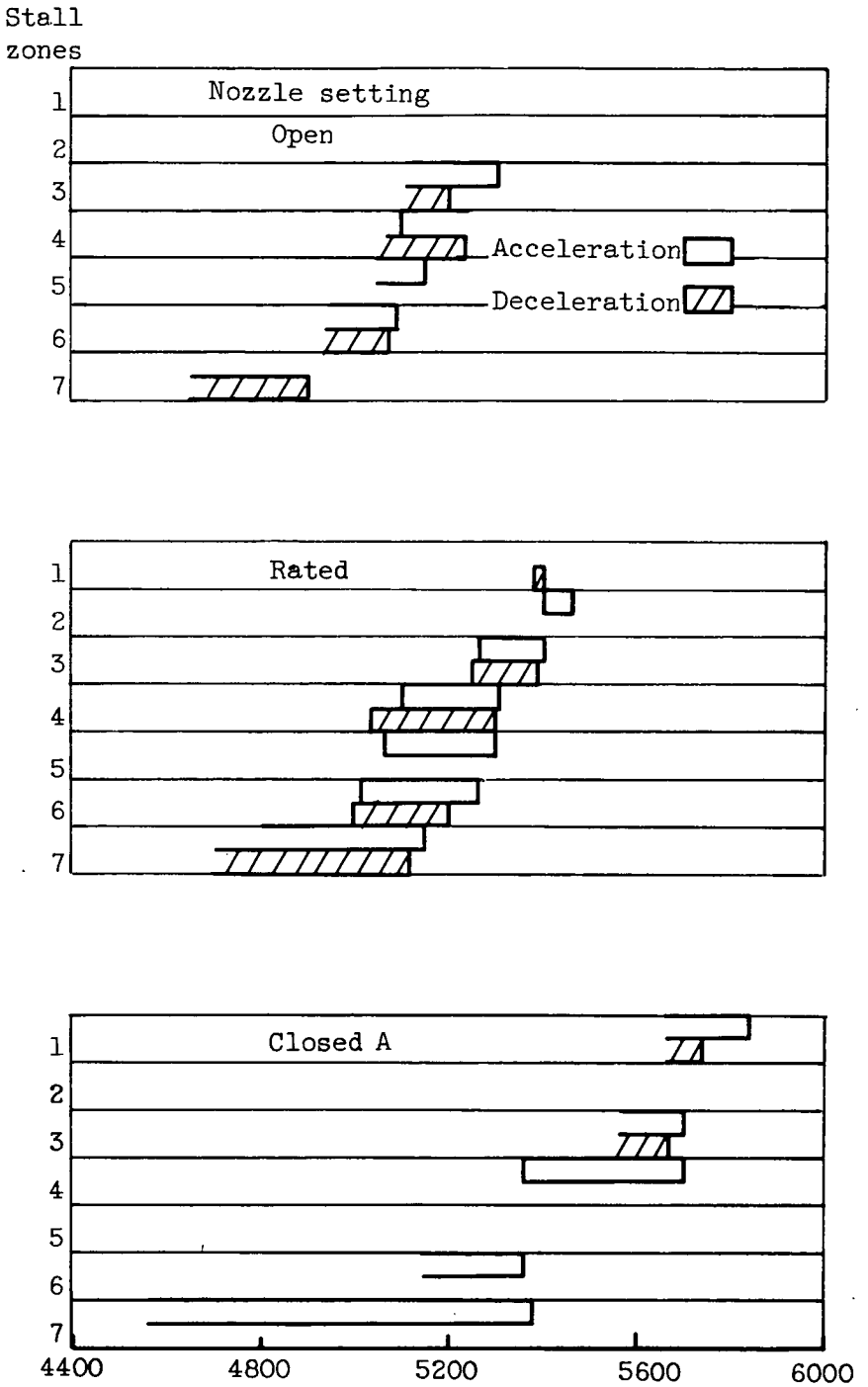

Figure 2. - Rotating-stall range for given number of zones with open, rated, and closed A nozzle.

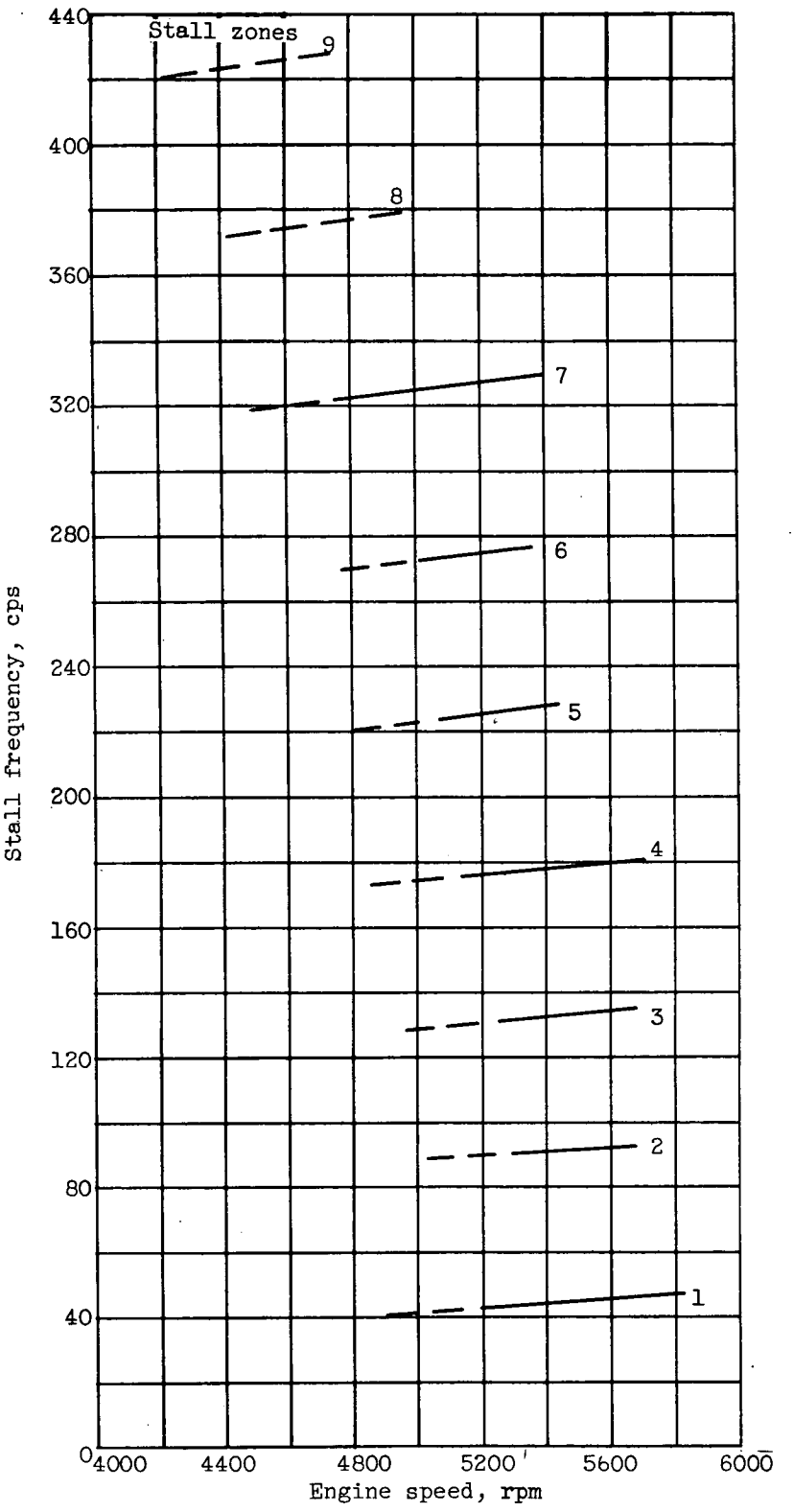

Figure 3. - Stall frequency against engine speed.

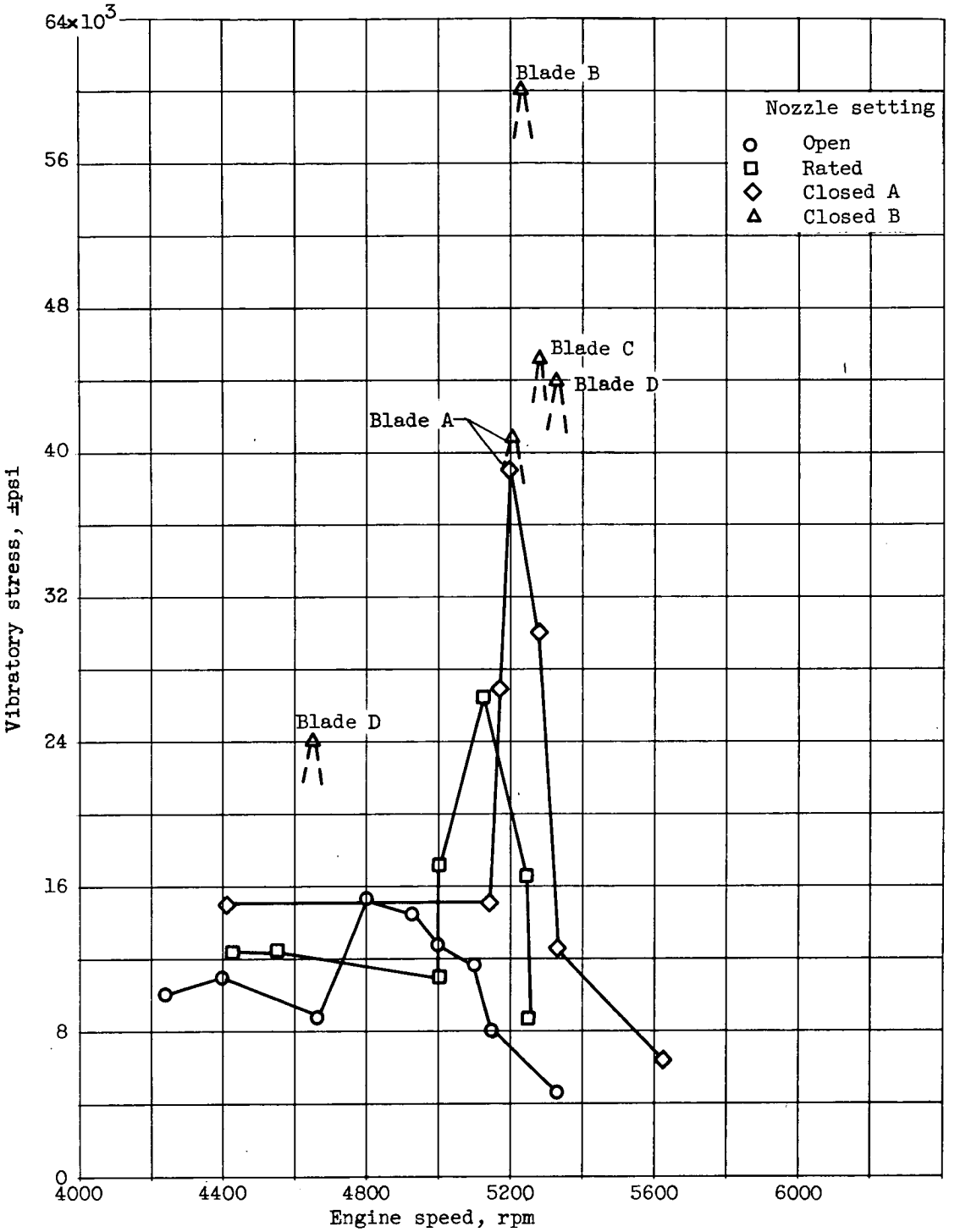

Figure 4. - Variation of vibratory stress with engine speed at various nozzle settings.

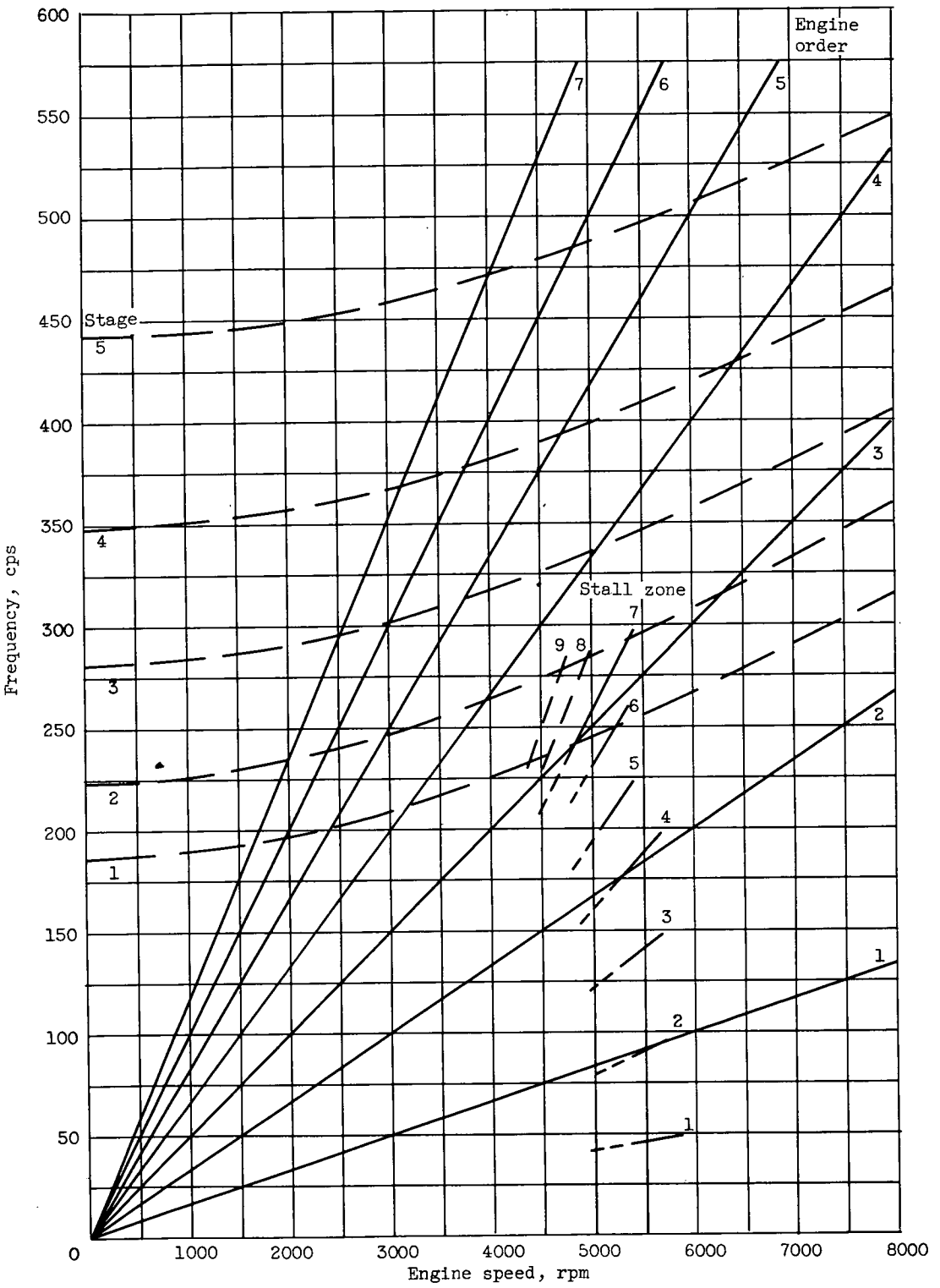

(a) Variation of natural blade frequency with engine speed.

Figure 5. - Order diagrams.

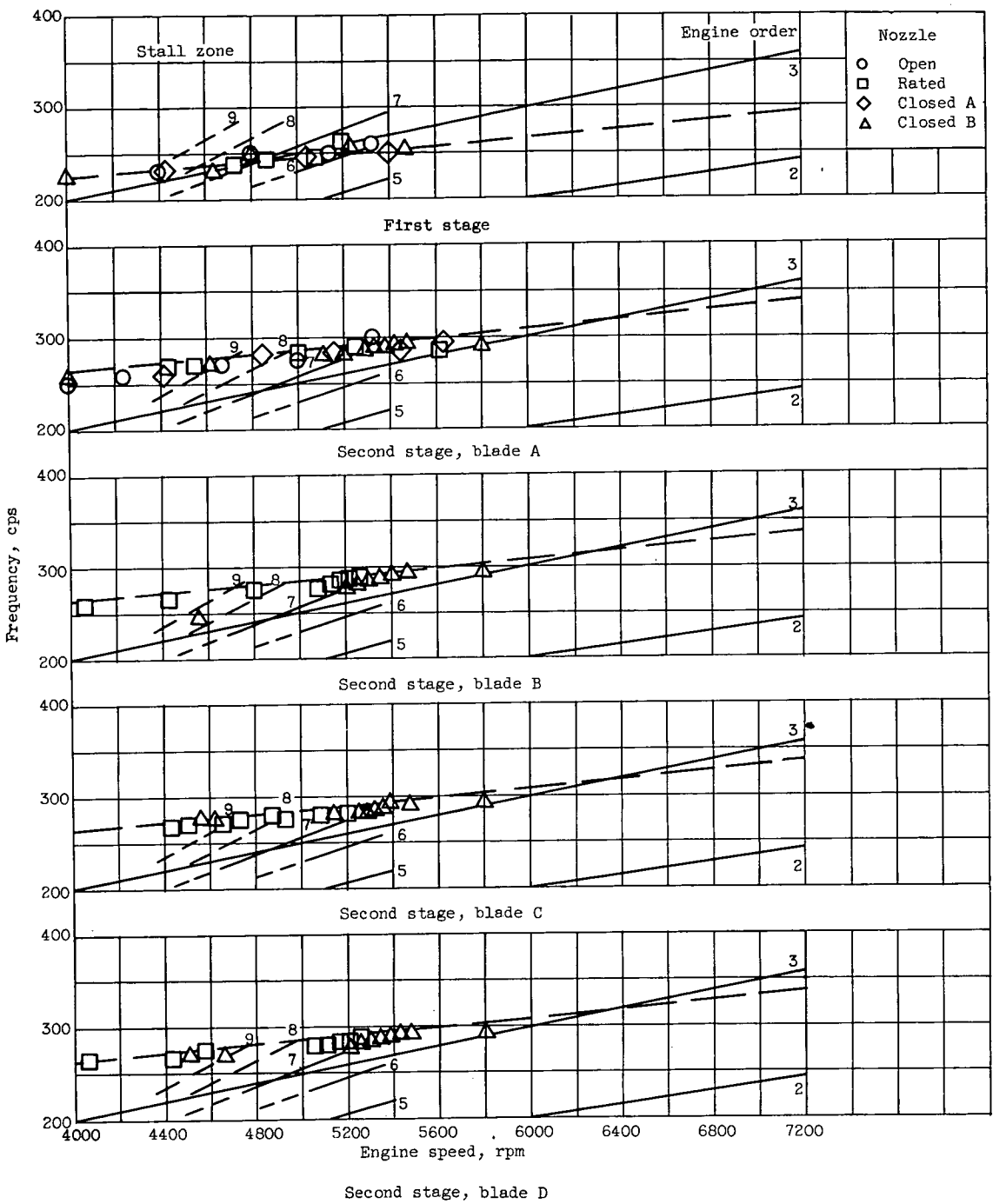

(b) Expanded variation of natural blade frequency with engine speed.

Figure 5. - Concluded. Order diagrams.

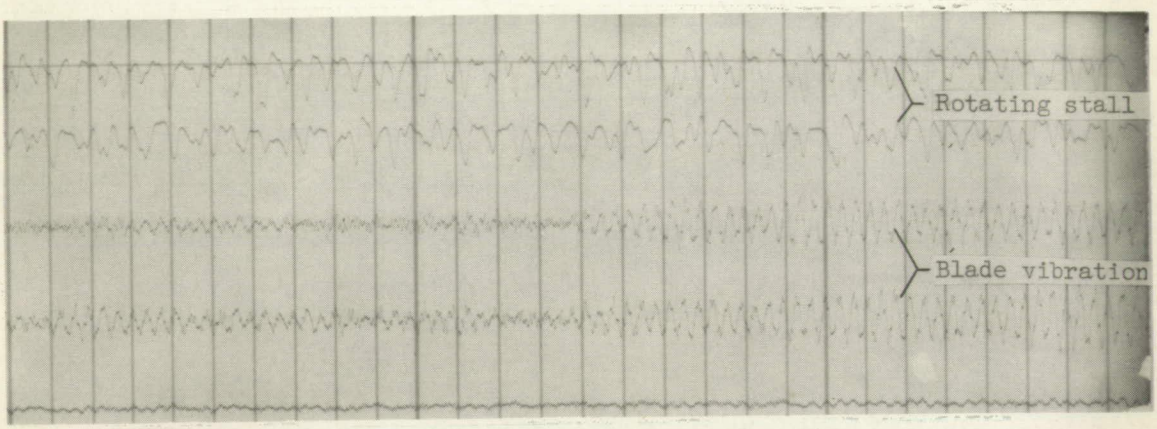

(a) Rated nozzle.

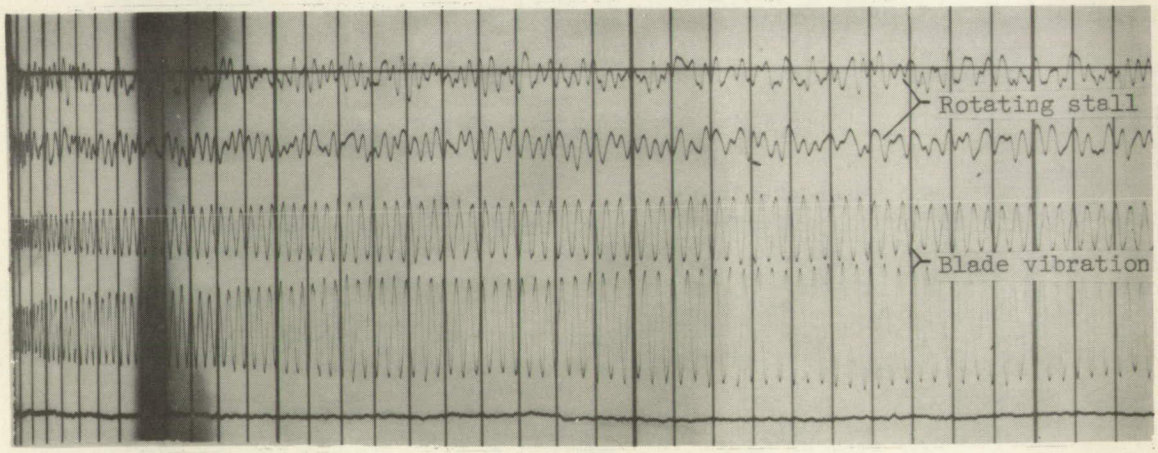

(b) Closed nozzle.

Figure 6. - Comparison of oscillograms of hot-wire and strain-gage signals with rated and closed nozzle at 5250 rpm.

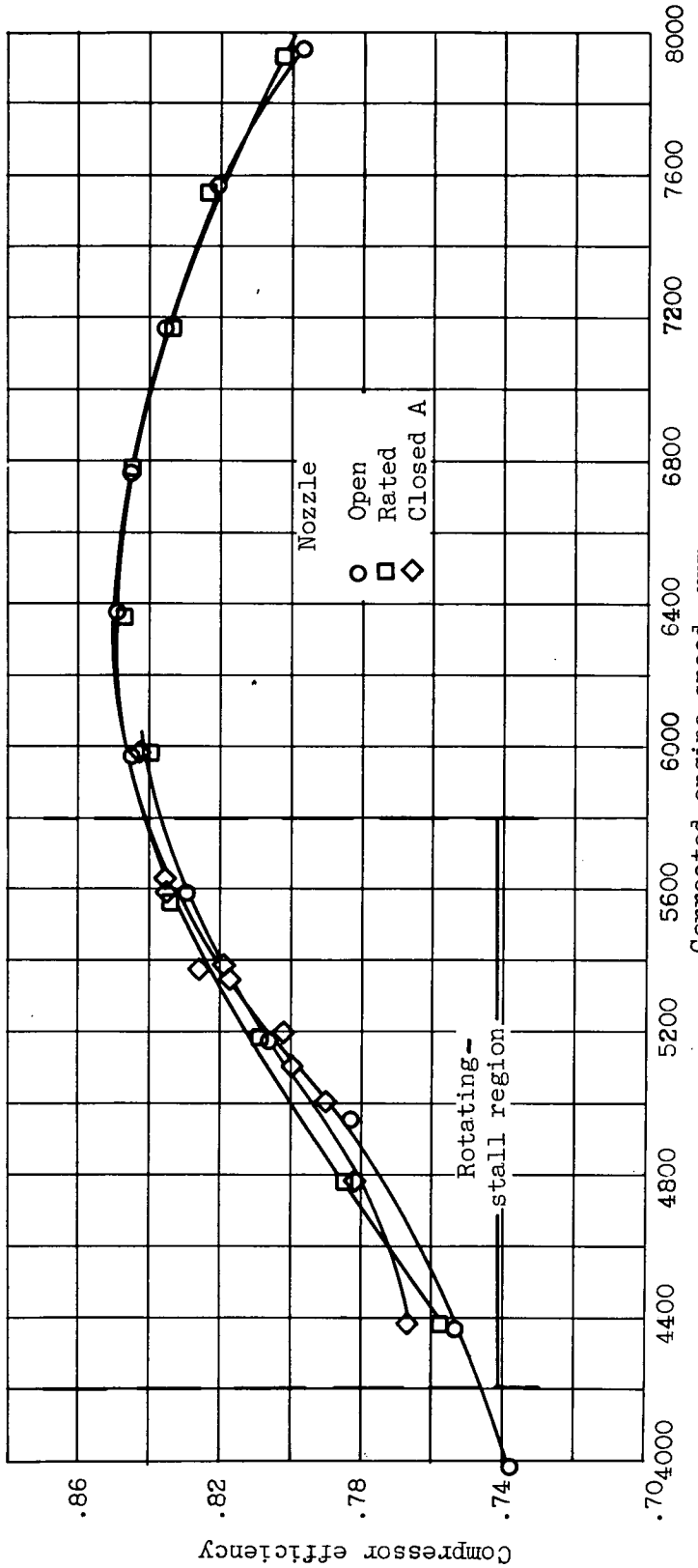

Figure 7. - Variation of efficiency with corrected engine speed.

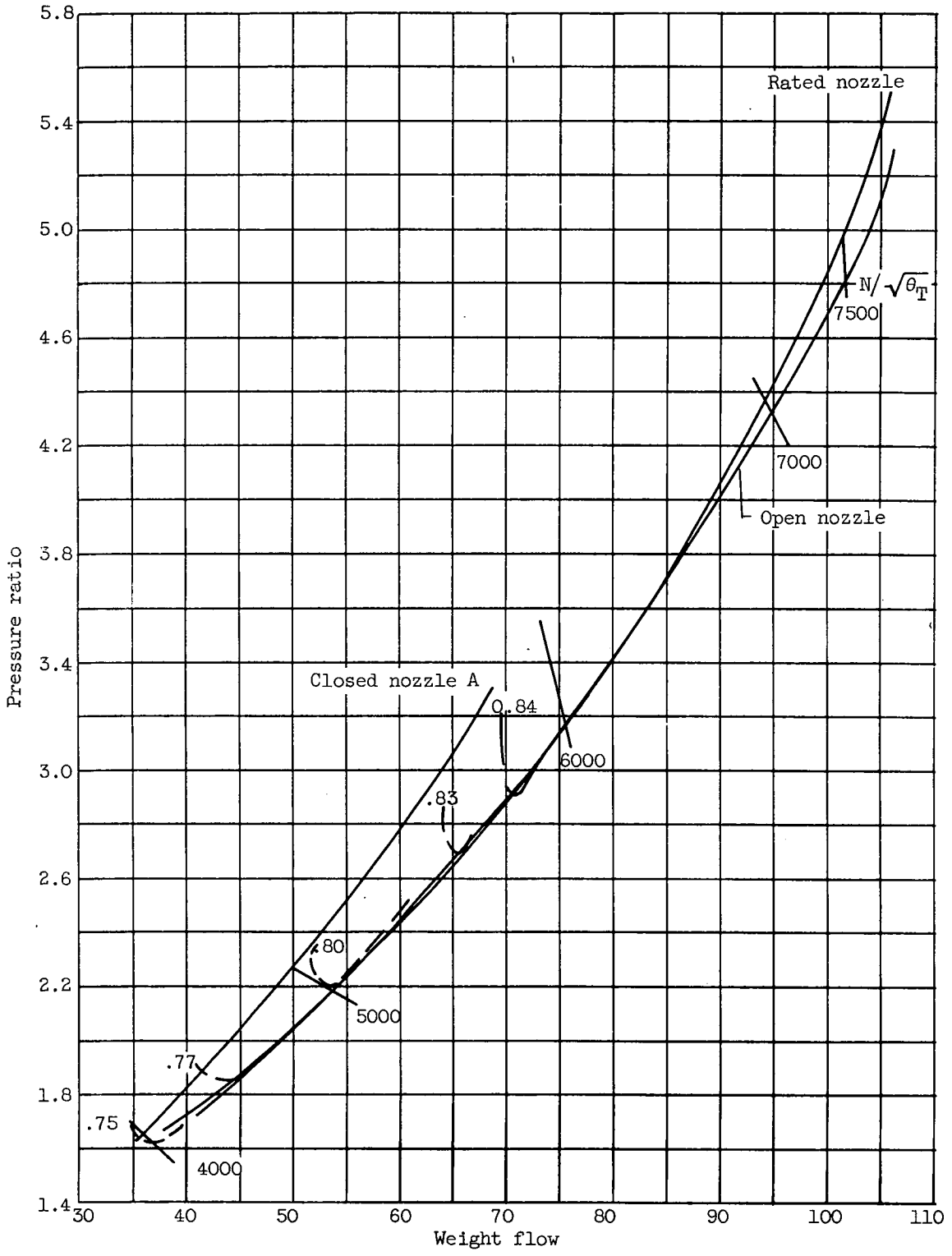

Figure 8. - Over-all performance of compressor.

NACA-Langley - 6-3-55 - 350